Aberration estimation using EUV mask roughness

Rene A. Claus[a], Antoine Wojdyla[b], Markus P. Benk[b], Kenneth A. Goldberg[b], Andrew R. Neureuther[c], Patrick P. Naulleau[b], and Laura Waller[c]

[a]Applied Science and Technology, University of California, Berkeley;
[b]Center for X-ray Optics, Lawrence Berkeley National Laboratory;
[c]EECS, University of California, Berkeley

ABSTRACT

We present a method to extract aberrations from through-focus aerial images of mask roughness on an Extreme Ultraviolet (EUV) lithography mask. The algorithm uses a phase recovery algorithm based on the Weak Object Transfer Function to recover the phase and amplitude of the roughness, while considering aberrations and partially coherent illumination. Using the self-consistency of the recovered object, aberrations, and measured images as a metric, we optimize over the space of aberrations to estimate aberrations. Partially coherent illumination is needed to allow the effects of the object field and aberrations to be separated. We apply the algorithm to the EUV aerial image microscope, SHARP, using a parameterized ray tracing model to calculate the aberrations from a lower dimensional parameter space.

Keywords: Extreme Ultraviolet Lithography, Mask Roughness, Aberration Recovery, Quantitative Phase Imaging

1. INTRODUCTION

In some situations, it may be difficult to align optics or measure aberrations in a microscope using standard techniques such as interferometry or Shack-Hartman. An alternative approach is to measure the phase of the wavefront using other phase retrieval techniques and extract the aberrations. One way to recover aberrations this way is to take images of a known object, such as contacts, through focus and attempt to find aberrations that explain the measurements using optimization.[1,2] Since this approach only requires a model that describes forward imaging in the microscope and a known object to be imaged, it can be used to align and evaluate a microscope without the need for modifications.

We present a similar algorithm that relaxes the requirement to have a known test object. We show that under partially coherent illumination it is possible to separate the imaging contributions of aberrations and of the object. Using a phase retrieval algorithm we have developed that is able to consider aberrations and partial coherence, we are able to find both the object and the aberrations that describe the measurements.[3,4] Our phase retrieval algorithm works on the assumption that the the object is weakly scattering, implying that the 0^{th} diffracted order dominates. Since EUV multilayer roughness is a perturbation on an ideal mirror it strongly satisfies this assumption.[5]

We applied the algorithm to measurements of EUV multilayer roughness conducted using the SHARP microscope at Lawrence Berkeley National Laboratory.[6] Due to field varying aberrations and image movement caused by non-telecentricity, the algorithm was modified to calculate the aberrations for each aerial image using ray tracing. Instead of optimizing over individual aberrations, the modified algorithm optimized over the position and orientation of the zone plate to reduce the number of parameters and to handle how aberrations change with focus.

Further author information: (Send correspondence to Rene A. Claus)
Rene A. Claus: E-mail: reneclaus@gmail.com, Telephone: 1 949 334 7363

Extreme Ultraviolet (EUV) Lithography VI, edited by Obert R. Wood II, Eric M. Panning,
Proc. of SPIE Vol. 9422, 942214 · © 2015 SPIE · CCC code: 0277-786X/15/$18
doi: 10.1117/12.2087513

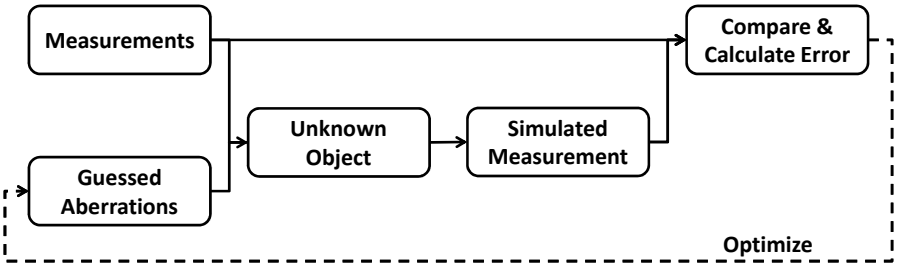

Figure 1. The algorithm consists of an outer optimization to minimize the residual error between the actual and simulated measurements (using an estimate of the object). At each step of the optimization, aberrations are assumed and an estimate of the object is recovered from the measurements.

2. ALGORITHM

Given through-focus images from a microscope with unknown aberrations, it is possible to simulate corresponding images by assuming particular aberrations. Using the difference between the simulated measurements and the actual measurements as a metric (we use the L2 norm between the stack of images), it is possible to perform an optimization (such as gradient descent) to find the aberrations that best match the measurements. This approach requires the object being imaged to be known. A more flexible approach allows the object to be arbitrary and uses the measurements and a quantitative phase retrieval algorithm to recover the object from the measurements during each step of the optimization. This approach is shown in Figure 1. A thin mask simulator can be used to calculate the simulated measurements.

There are two challenges in the proposed algorithm:

1. The phase retrieval algorithm needs to consider the currently guessed aberrations.
2. In coherent imaging the object and aberrations are not separable.

We have developed a new phase retrieval algorithm based on the weak object transfer function that works with through-focus images taken with arbitrary source shapes while fully considering an arbitrary pupil. A more detailed explanation of the algorithm is being prepared.[4,7] The limitation of this algorithm is that the object needs to be weakly scattering (have a strong DC component). Phase roughness resulting from replicated multilayer roughness on EUV masks is an excellent test object—it is readily available on masks and satisfies the algorithm requirement well.

The ability to consider partially coherent illumination is critical to distinguishing the effect of the object on the measurements from the effect of the aberrations. The reason is that under coherent illumination the intensity measured is $I = |E * P|^2$, where E is the scalar electric field at the mask and P is the coherent point spread function. If both P and E are unknown, there is no way to distinguish this case from $I = |E' * P'|^2$ where E' and P' are some other electric field and pupil function. Effectively, under coherent illumination it is only possible to measure the field at the camera and not at the wafer. At that point the aberrations and object have already been combined. This problem disappears when partially coherent illumination is used because the object sees a shifted pupil function for each illumination angle. Figure 2 shows the residual error for different assumed amounts of astigmatism when the algorithm is applied to simulated through focus measurements. The goal of the optimization is to find the minimum of this curve. Twenty one through-focus images of phase roughness were simulated for defocus in the range $\pm 5\ \mu m$. The simulation used a true astigmatism value of 0.1λ RMS. In the case of coherent illumination there is no way to find the correct aberration—no matter what astigmatism is assumed, the algorithm is able to find an object that explains the measurements. Once partially coherent illumination is used, however, there is a minimum in the residual for the correct aberration. Notice that as the illumination becomes less coherent ($\sigma = 0.5$ vs. $\sigma = 0.2$) the residual becomes more sensitive to the aberrations indicated by a lower sharper minimum in the residual.

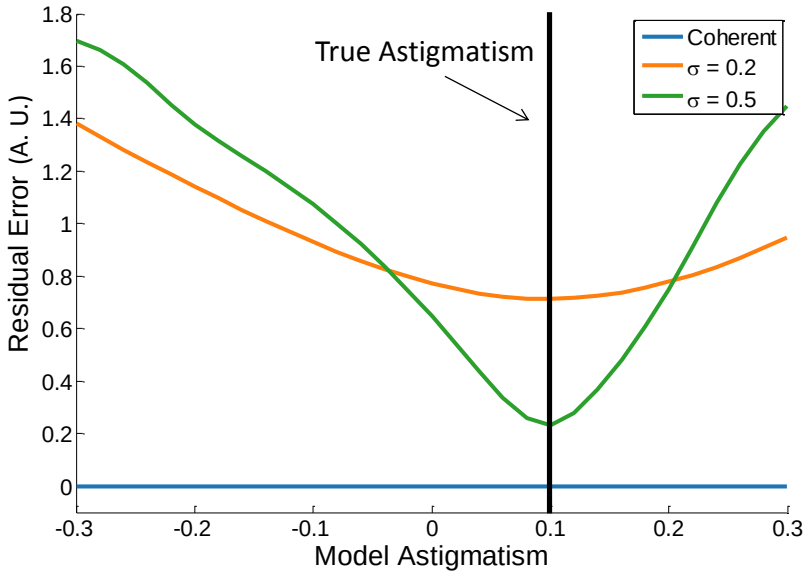

Figure 2. Under coherent illumination the object and aberrations are linearly dependent and can not be distinguished. Once partially coherent illumination is used it becomes possible to separate the two as indicated by the residual curves. Less coherent illumination causes a stronger sensitivity to aberrations in the proposed algorithm.

3. EXPERIMENT

We applied this algorithm to data collected on the SHARP EUV mask imaging microscope. SHARP uses a single off-axis zone plate as the objective lens, resulting in two complications in the imaging characteristics:

1. The image of the object moves across the camera as focus is varied because the system uses an off-axis zone plate and off-axis illumination.
2. There are strong field dependent aberrations away from the center of the field because the system uses a single imaging lens.

These two problems together mean that the aberrations that affect a particular patch of roughness are not constant but change with focus. Since the algorithm described above considers aberrations to be constant while focus is varied, we modified the algorithm slightly. Instead of considering aberrations directly we model the zone plate physically and calculate the aberrations for each image by ray tracing using physical parameters such as the tip, tilt, and x, y, and z shifts of the zone plate. This reduces the number of parameters, making the optimization more constrained and incorporates how the aberrations change with focus. A small patch of the image (100×100 pixels at 15 nm / pixels) away from the center of the field was considered so that the aberrations could be assumed to not vary across the patch. A sample of such a patch is shown in Figure 3. The pupil function is calculated for the center of the patch in each image. An entire measured stack of 21 images with 500 nm focus steps was used. The numerical aperture (NA) was 0.0825 corresponding to a 0.33 wafer side NA, the wavelength 13.5 nm, and the illumination was a monopole with $\sigma = 0.25$.

Automatic optimization failed to converge to a reasonable and consistent position and orientation of the zone plate. We believe that the most likely reasons for this failure are field-varying illumination and stage drift, which were not considered in the model. If the assumed illumination or image alignment are incorrect the minimum that the optimization searches for will move and the algorithm will return an incorrect answer. The model could be extended to include these effects, but this also creates more local minima potentially making the optimization more difficult.

Although automatic optimization failed to produce good results in general, manually selecting values for the position and orientation of the zone plate showed some ability to calibrate the system. After manually selecting

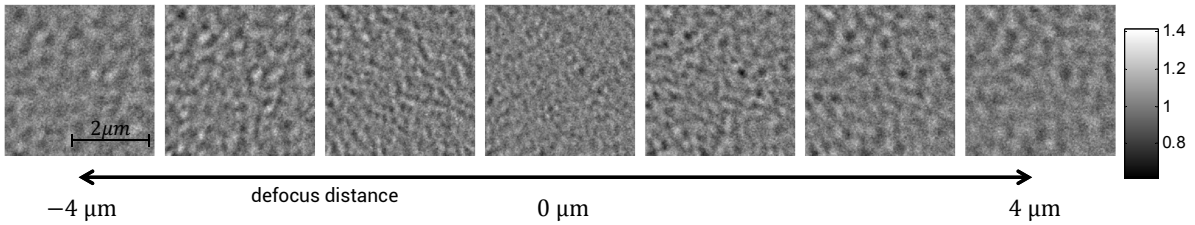

Figure 3. A subset of through-focus aerial images of roughness measured on SHARP. This roughness is 10 μm from the center of the field.

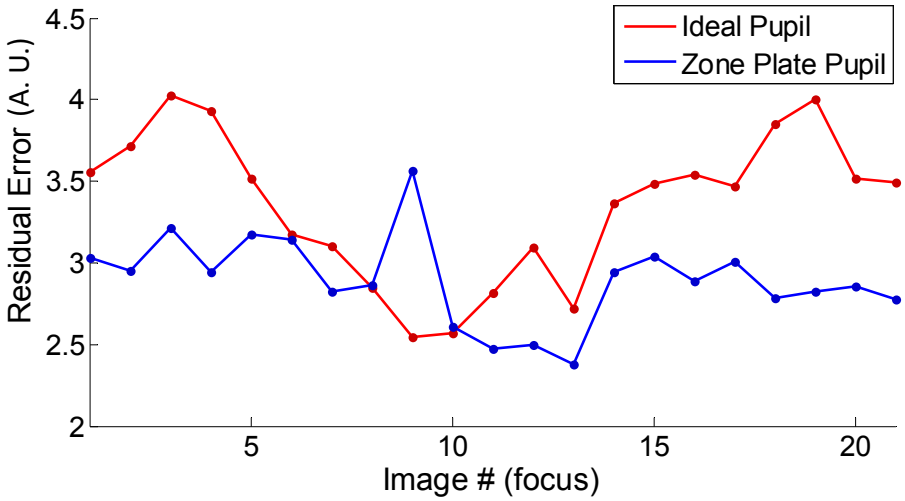

Figure 4. The residual for each image is plotted for an ideal pupil that considers only defocus and no aberrations, as well as for the zone plate model that was manually optimized. The zone plate model performs better especially at the edges of the focus stack where aberrations are varying the most.

and testing likely parameter values, the residual was noticeably improved. Figure 4 shows the per-image residual for all the images in the stack after manual optimization for the physical zone plate model and for the case of an ideal pupil that considers only defocus and no aberrations. The error is generally lower for the zone plate model. The ideal pupil case fits well at the center of the stack, but as the aberrations change towards the ends of the focus series the fit becomes worse. This is because the phase recovery is able to incorporate some of the aberrations into the object. The aberrations incorporated are expected to be close to the average aberration among the images in the stack.

Figure 5 shows the recovered amplitude and phase for each model and their power spectral densities (PSD). There is a directional component in the field (most apparent in the amplitude PSD) that is likely due to aberrations being incorporated into the object. This effect is stronger for the ideal pupil case where aberrations are not being considered in the pupil function. The uncorrected aberrations are even more apparent when looking at the residual images directly. Figure 6 shows one image from the focus stack and the simulated image for each model. Notice that the residual PSD has a relatively strong directional component for the ideal pupil that is not present for the zone plate model. This indicates that the ray tracing model is removing that aberration.

4. CONCLUSION

We have proposed a way to extract aberrations from through-focus aerial images without the need for a known test object. We use partially coherent illumination to allow the pupil and object to be separated. To recover the object field we use a quantitative phase recovery algorithm based on the weak object approximation. The requirement of the algorithm to use a weakly scattering object makes EUV mask roughness an excellent test

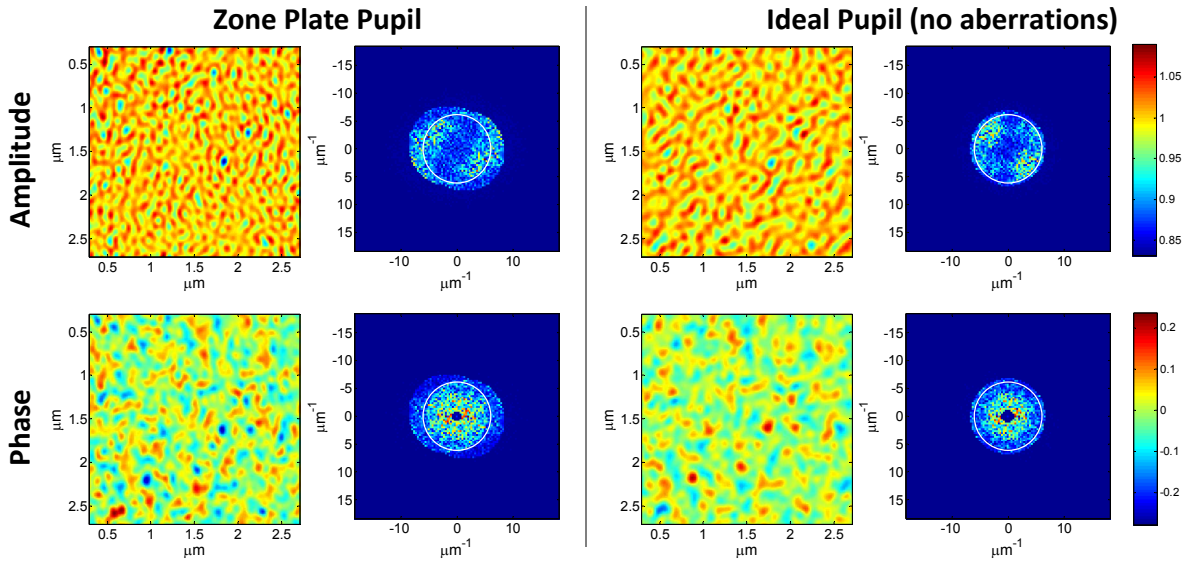

Figure 5. The recovered amplitude and phase and their corresponding PSDs are shown for the case of the zone plate model and the ideal pupil. The different recovered frequencies in the case of the zone plate model resulted from considering how the NA shifted geometrically in the measurements.

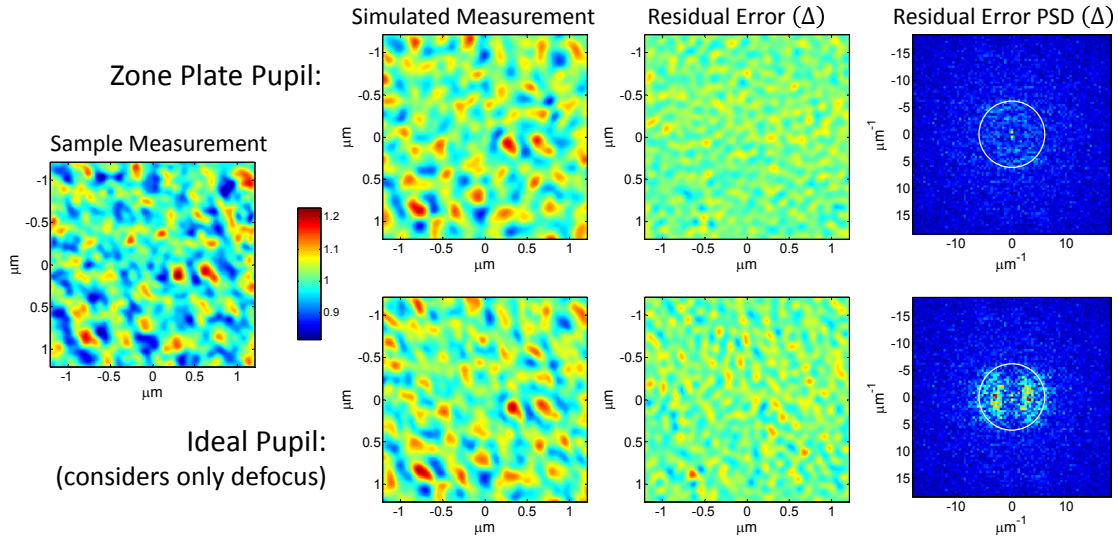

Figure 6. One image from the stack of images is illustrated. The corresponding simulated image, residual, and residual PSD are shown for the zone plate model and the ideal pupil case. The ideal pupil failed to account for aberrations present in the image. This is visible in the residual PSD.

object. The aberrations are found by minimizing the residual between the measurements and corresponding images simulated using the recovered object.

We applied the algorithm to data taken on the EUV microscope SHARP using a ray tracing model to calculate the field dependent aberrations. Automatic optimization encountered problems due to local minima, but manual optimization showed that the zone plate model is able to remove aberrations.

ACKNOWLEDGMENTS

This work performed in part at Lawrence Berkeley National Laboratory which is operated under the auspices of the Director, Office of Science, of the U.S. Department of Energy under Contract No. DE-AC02-05CH11231. This research was supported by collaboration with industry under the IMPACT+ program (`http://impact.ee.ucla.edu`).

REFERENCES

[1] Paxman, R. G., Schulz, T. J., and Fienup, J. R., "Joint estimation of object and aberrations by using phase diversity," *J. Opt. Soc. Am. A* **9**, 1072 (July 1992).

[2] Yamazoe, K., Mochi, I., and Goldberg, K. A., "Gradient descent algorithm applied to wavefront retrieval from through-focus images by an extreme ultraviolet microscope with partially coherent source," *J. Opt. Soc. Am. A* **31**(12), 34–43 (2014).

[3] Claus, R. A., Mochi, I., Benk, M. P., Goldberg, K. A., Neureuther, A. R., and Naulleau, P. P., "Recovering effective amplitude and phase roughness of EUV masks," *Proc. SPIE* **8880**, 88802B–88802B–7 (2013).

[4] Claus, R. A., Naulleau, P. P., Neureuther, A. R., and Waller, L., "Quantitative phase retrieval algorithm for arbitrary pupil and illumination," (2015). in submission.

[5] George, S. A., Naulleau, P. P., Gullikson, E. M., Mochi, I., Salmassi, F., Goldberg, K. A., and Anderson, E. H., "Replicated mask surface roughness effects on euv lithographic patterning and line edge roughness," (2011).

[6] Goldberg, K. A., Mochi, I., Benk, M., Allezy, A. P., Dickinson, M. R., Cork, C. W., Zehm, D., Macdougall, J. B., Anderson, E., Salmassi, F., Chao, W. L., Vytla, V. K., Gullikson, E. M., DePonte, J. C., Jones, M. S. G., Van Camp, D., Gamsby, J. F., Ghiorso, W. B., Huang, H., Cork, W., Martin, E., Van Every, E., Acome, E., Milanovic, V., Delano, R., Naulleau, P. P., and Rekawa, S. B., "Commissioning an EUV mask microscope for lithography generations reaching 8 nm," *Proc. SPIE* **8679**, 867919–867919–10 (2013).

[7] Claus, R. A., Wang, Y.-G., Wojdyla, A., Benk, M., Goldberg, K., Neureuther, A. R., Naulleau, P. P., and Waller, L., "Phase Measurements of EUV Mask Defects," *Proc. SPIE* **9422** (2015).